International Journal of Pharmaceutics, 78 (1992) 123–136

IJP 02596

Assessing the influence of ethanol on simultaneous diffusion and metabolism of β-estradiol in hairless mouse skin for the 'asymmetric' situation in vitro

Puchun Liu [1], William I. Higuchi [1], Abdel-Halim Ghanem [1], Tamie Kurihara-Bergstrom [2] and William R. Good [1,2]

[1] *Department of Pharmaceutics, University of Utah, Salt Lake City, UT 84112 (U.S.A.) and* [2] *Pharmaceuticals Division, Ciba-Geigy Corporation, Ardsley, NY 10502 (U.S.A.)*

(Received 12 December 1990)
(Modified version received 1 August 1991)
(Accepted 2 August 1991)

Key words: Vehicle effect; Asymmetric model; Ethanol flux; Ethanol gradient; β-Estradiol flux; β-Estradiol gradient; β-Estradiol metabolism; Hairless mouse skin

Summary

A novel theoretical model/method has been developed to predict permeant transport across skin for the 'asymmetric' case, i.e., for situations in which there is significant cotransport of an enhancer solvent along with the principal permeant. The method has successfully predicted effects of the simultaneous transport of ethanol on the simultaneous diffusion and metabolism of β-estradiol ($E_{2\beta}$) at steady state in hairless mouse skin using parameter values deduced from experiments conducted under symmetric conditions (i.e., the same ethanol concentration on both sides of the skin membrane). The studies have involved the determination of (a) effective ethanol concentration gradients and (b) skin position-dependent permeability coefficients and partition coefficients, concentration (activity) gradients, and fluxes for $E_{2\beta}$ and its transdermal metabolite, estrone (E_1), with stripped skin and with full thickness skin. As this approach is quite general and as the asymmetric situation is the practical situation in vivo, it is believed that the outcomes of this study are important in transdermal/dermal formulations research.

Introduction

The present research was undertaken because there is a need for general in vitro approaches for dealing with the many factors influencing dermal/transdermal transport and metabolism and because transdermal β-estradiol ($E_{2\beta}$) delivery systems are of current interest. Recently (Liu et al., 1990), baseline in vitro studies on the transport and metabolism [$E_{2\beta} \rightarrow$ estrone (E_1)] with hairless mouse skin were completed. The experiments were carried out in a two-chamber diffusion cell system with saline in both chambers, using full-thickness skin, stripped skin, and dermis and the data were analyzed via several physical models. A 'best' model was deduced in which skin is considered to be a three-layer membrane (stratum corneum, epidermis, and dermis) with

Correspondence: W.I. Higuchi, Department of Pharmaceutics, University of Utah, Salt Lake City, UT 84112, U.S.A.

the metabolizing enzyme activity totally residing in the epidermis and near the basal layer (i.e., near the dermo-epidermal junction).

These studies were very recently extended to the case in which aqueous ethanol was present in both the donor and receiver chambers at equal concentrations (i.e., the 'symmetric' situation) up to 25% (v/v). At these low to moderate concentrations, ethanol was found to have two effects: (a) ethanol acts as a stratum corneum penetration enhancer for $E_{2\beta}$ and E_1 and (b) ethanol is able to retard or inhibit the $E_{2\beta} \rightarrow E_1$ enzyme reaction (Liu et al., 1991).

The purpose of this paper is to describe the results of further studies, those involving the practically significant situation where aqueous ethanol is present in the donor chamber with saline only in the receiver chamber (i.e., the asymmetric situation). A strategy is employed here where the experimental results for the asymmetric situation are analyzed in terms of the parameter values deduced from the symmetric ethanol experiments. It is believed that the outcomes have general and broad utility in that the methods developed may be applied to other drug/vehicle situations where there is cotransport of an excipient that may act as a stratum corneum permeation enhancer (Mollgaard and Hoelgaard, 1983a,b; Higuchi et al., 1985, 1987; Kurihara-Bergstrom et al., 1986; Sarpotdar et al., 1986; Sloan et al., 1986; Ghanem et al., 1987).

Theoretical Basis of the Method

The general problem of predicting the effects of ethanol in the asymmetric situation on the diffusion and metabolism of $E_{2\beta}$ in the skin is illustrated in Fig. 1 where the concentration profiles for ethanol, $E_{2\beta}$, and E_1 (the metabolite) in the stratum corneum (S.C.), the epidermis (Epid.), and dermis are schematically presented. For the purpose of the discussion to follow, we will assume that steady-state conditions prevail and, therefore, that the concentration profiles for the three species presented in Fig. 1 are steady-state concentrations in the skin. First, as expected (and will be shown later), the main concentration drop for ethanol occurs across the stratum corneum; therefore, for the conditions of the experiments to be reported here, the influence of ethanol upon the $E_{2\beta}$ diffusion coefficient and the $E_{2\beta}$ partition coefficient in the epidermis and in the dermis would be expected to be negligible. How-

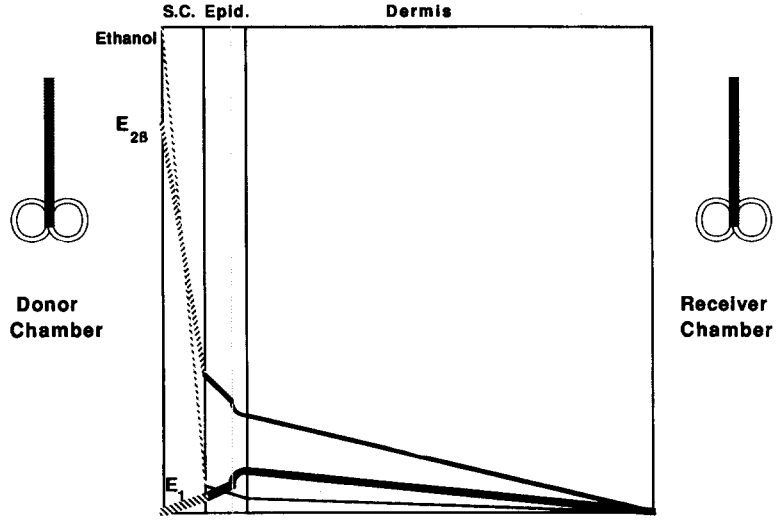

Fig. 1. Schematic representations of concentration profiles for ethanol, $E_{2\beta}$ and E_1 (the metabolite) in the stratum corneum (S.C.), the epidermis (Epid.), and dermis of hairless mouse skin in the simultaneous diffusion and metabolism of $E_{2\beta}$ in the asymmetric situation (ethanol gradient across the skin).

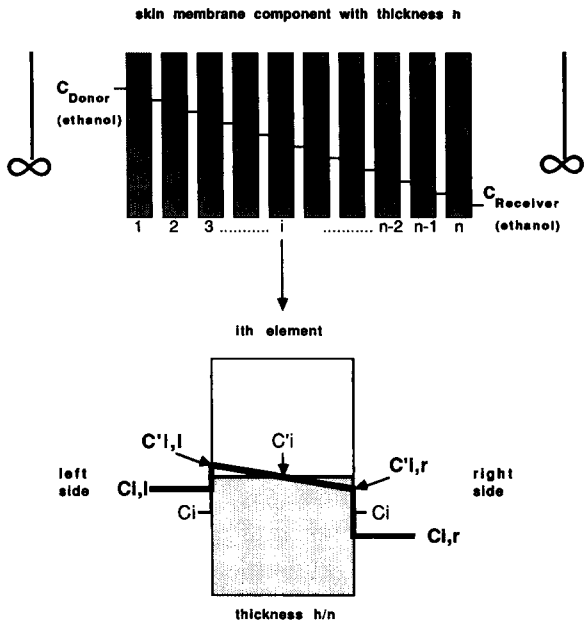

Fig. 2. Physical model of diffusion for the asymmetric (ethanol) situation.

ever, in the epidermis, the ethanol levels may be expected to be high enough to reduce the rate of $E_{2\beta}$ metabolism to E_1. With regard to $E_{2\beta}$, the transport of $E_{2\beta}$ in the stratum corneum is expected to be strongly dependent upon the steady-state ethanol concentration profile. As the transport enhancement of $E_{2\beta}$ in the skin is a function of the ethanol concentrations (Ghanem et al., 1987; Liu et al., 1991), the ethanol gradient in the stratum corneum is expected to cause a position-dependent (i.e., in the stratum corneum) enhancement of $E_{2\beta}$ transport. Fig. 1 also illustrates the E_1 concentration profile which results from the $E_{2\beta}$ metabolism in the epidermis (mostly, the basal layer near the dermo-epidermal junction; see Liu et al., 1991). The back diffusion of E_1 into the donor chamber is also expected to be enhanced by the ethanol gradient in the stratum corneum.

Fig. 2 illustrates the general problem in which a steady-state concentration gradient of ethanol is present across a skin membrane component. Here, the membrane with thickness h is regarded as being made up of n elements (with the same thickness, h/n). It will be assumed for mathematical purposes that there is a thin layer of the aqueous ethanol solution between any two neighboring elements, i.e., each element is sandwiched between the two hypothetical aqueous ethanol solutions that are at slightly different ethanol concentrations. In the steady state, the flux (J) through the i-th layer is the same as those for other layers and is given by:

$$J = \frac{D_i}{\left(\frac{h}{n}\right)}(C'_{i,l} - C'_{i,r}) \tag{1}$$

where D_i is the average diffusion coefficient for the permeant in element i, and $C'_{i,l}$ and $C'_{i,r}$ are the permeant concentrations at the left and right interfaces of element i, respectively. We may further write,

$$C'_{i,l} = K_{i,l}C_{i,l}$$

and (2)

$$C'_{i,r} = K_{i,r}C_{i,r}$$

where $K_{i,l}$ and $K_{i,r}$ are the element-to-solvent (aqueous ethanol solution) partition coefficients at the left and right sides of element i, respectively, and $C_{i,l}$ and $C_{i,r}$ are the permeant concentrations in the hypothetical solvents (aqueous ethanol solutions) on the left and right sides of element i, respectively. Combining Eqns 1 and 2, we have

$$J = \frac{D_i}{\left(\frac{h}{n}\right)}(K_{i,l}C_{i,l} - K_{i,r}C_{i,r}) \tag{3}$$

Eqn 3 may then be rearranged to give

$$J = \frac{D_i}{\left(\frac{h}{n}\right)}K_i\left[\left(\frac{K_{i,l}}{K_i}\right)C_{i,l} - \left(\frac{K_{i,r}}{K_i}\right)C_{i,r}\right] \tag{4}$$

where K_i is the partition coefficient for the element at the average ethanol concentration (see Fig. 2).

The average permeability coefficient may now be defined for the element i,

$$P_i = \frac{D_i K_i}{\left(\frac{h}{n}\right)} \tag{5}$$

Then Eqn 4 becomes

$$J = P_i\left[\left(\frac{K_{i,l}}{K_i}\right)C_{i,l} - \left(\frac{K_{i,r}}{K_i}\right)C_{i,r}\right] \tag{6}$$

Eqn 6 may be used to predict fluxes and permeant concentration gradients for the several different situations. These will be ethanol transport across stripped skin and full-thickness skin for the asymmetric situation and $E_{2\beta}$ transport and metabolism for the asymmetric situation with stripped skin and full-thickness skin.

The calculations are easily carried out when the P_i values and the ratios of the partition coefficients ($K_{i,l}/K_i$ and $K_{i,r}/K_i$) are known for the permeants as functions of the ethanol concentration. For these theoretical calculations, it is assumed that each membrane component (e.g., the dermis, epidermis, and the stratum corneum) may be divided into n equal elements. The solution then basically involves finding the correct J value; this is simply the J value for which the boundary conditions (i.e., the donor and the receiver chamber concentrations of the permeant) are obeyed.

For the case of $E_{2\beta}$ as the permeant, Eqn 6 is no longer applicable to the basal cell layer simultaneous diffusion and metabolism ($E_{2\beta} \rightarrow E_1$); for this situation, the following modified equations must be numerically solved in the basal layer (Liu, 1989),

$$\frac{d\left[D_{2\beta}(x)\frac{dC_{2\beta}}{dx}\right]}{dx} - k(x)C_{2\beta} = 0 \tag{7}$$

$$\frac{d\left[D_1(x)\frac{dC_1}{dx}\right]}{dx} + k(x)C_{2\beta} = 0 \tag{8}$$

where $C_{2\beta}$ and C_1 are the concentrations of $E_{2\beta}$ and of E_1, $D_{2\beta}(x)$ and $D_1(x)$ are the position-dependent diffusion coefficients of $E_{2\beta}$ and of E_1, and $k(x)$ is the position-dependent enzyme rate constant.

Experimental

Materials

Chemical materials $E_{2\beta}$ and E_1 (Sigma Chemical Co., St Louis, MO) were used to make the standard mixtures in methanol (Baker Chemical Co., Phillipsburg, NJ). Normal saline (McGaw, Irvine, CA) and pure ethanol (US Industrial Chemical Co., Tuscola, IL) were used to prepare the solvent mixtures for all experiments. Analytical grade acetonitrile (Baker Chemical Co., Phillipsburg, NJ) was used in the preparation of the HPLC mobile phase. Liquid scintillation fluid, Ready-Solv CP (Beckman Institute, San Ramon, CA), was used as obtained commercially. [6,7-^{3}H]$E_{2\beta}$ (60.0 Ci/mmol) was obtained in ethanol solutions from New England Nuclear, Boston, MA. The ethanol was evaporated with the aid of a nitrogen stream before [^{3}H]$E_{2\beta}$ was used for diffusion/metabolism experiments. [^{14}C]Ethanol (30 mCi/mmol) was obtained commercially (New England Nuclear, Boston, MA) and diluted properly into the pure ethanol for ethanol diffusion experiments.

Skin membrane preparations Male hairless mice (strain SKH-HR1), age 12–15 weeks, were obtained from Temple University, Pittsburgh, PA. Mice were killed by spinal dislocation. Two pieces of skin preparation were obtained from the abdominal region of each mouse. Three kinds of fresh membranes (full-thickness skin, stripped skin, and dermis) were prepared. Full-thickness skin, consisting of stratum corneum, viable epidermis and dermis, was excised from the animal with surgical scissors. After the incision was made, the skin was lifted and the adhering fat and other visceral debris were carefully removed from the under surface. Stripped skin, consisting of the epidermis and the dermis, was obtained after the stratum corneum was removed by a cellophane tape (Scotch tape, 3M Co., St. Paul, MN) strip-

ping technique (Yu et al., 1979). Dermis was obtained by removing the epidermal half of the skin by using a dermatome (Yu et al., 1979). The dermis thickness was measured with a micrometer before and after the experiment by sandwiching the membrane between two glass slides (Yu et al., 1979). All of the dermis data were normalized for the full-thickness dermis with thickness of 250 μm (Liu et al., 1990).

Two-chamber diffusion cell The diffusion cell (Durrheim et al., 1980) was made up of two half chambers, each having a volume of 2 ml and an effective diffusional area of about 0.7 cm^2. In each chamber, a stainless-steel stirrer (for $E_{2\beta}$ experiments) or a plastic stirrer (for ethanol experiments) with a small stainless-steel propeller was driven by a 150 rpm constant speed motor. The thickness of the aqueous diffusion layer for a 150 rpm system was found to be 0.010 cm from a benzoic acid dissolution rate experiment (Yu et al., 1979). The aqueous boundary layer resistances were assessed to be negligible for ethanol, $E_{2\beta}$, and E_1 compared to their skin transport resistances (Stehle and Higuchi, 1972). For ethanol experiments (described below), the diffusion setup was placed in a hood.

Experimental methods

Ethanol diffusion experiments Both symmetric (same ethanol concentration in both chambers) and asymmetric (ethanol in donor chamber only, saline in the receiver) experimental arrangements were used for studying the diffusion of [^{14}C]ethanol. The [^{14}C]ethanol fluxes were measured with dermis, stripped skin, and full-thickness skin for various ethanol concentrations. The two-chamber diffusion cell procedure was employed with freshly excised hairless mouse dermis, stripped skin, and full-thickness skin. A skin membrane was mounted between the two chambers of the diffusion cell with the dermis side facing the receiver chamber, clamped and the excess skin trimmed. The assembled diffusion cells were immersed in a water bath at 37 °C. A predetermined level of [^{14}C]ethanol was added into the donor chamber and aliquots were withdrawn at predetermined time intervals after steady state was attained. In most of the experiments, 100-μl aliquots were taken from the receiver chamber and 5-μl aliquots from the donor chamber. The same volume of saline solution was added back to the receiver chamber; solvent was not added back to the donor chamber. Samples were analyzed by liquid scintillation counting (Beckman LS 750, Beckman Institute, San Ramon, CA). The apparent permeability coefficients were calculated from

$$P = \frac{J}{C_D} = \frac{\left(\frac{dC_R}{dt}\right)\frac{V_R}{S}}{C_D} \tag{9}$$

where V_R is the volume of the receiver chamber, S is the effective diffusion area, and C_D and C_R are the donor and receiver chamber concentrations, respectively, and dC_R/dt is the steady-state slope of the receiver concentration vs time curve.

$E_{2\beta}$ diffusion / metabolism experiments The two-chamber cell experiments with $E_{2\beta}$ were conducted with dermis, stripped skin, and full-thickness skin in both the symmetric and asymmetric situations. The experimental procedure was similar to that described in the ethanol diffusion experiments. Separation of [^{3}H]$E_{2\beta}$ or [^{3}H]E_1 was performed by interfacing the HPLC (high-performance liquid chromatograph) with a fraction collector (Liu et al., 1990). The HPLC system was a V4 Variable-Wavelength Absorbance Detector (ISCO, Lincoln, NE), a 110B Solvent Delivery Module (Beckman Institute, San Ramon, CA), and a C6W injector (Valco Institute, San Antonio, TX). The species were resolved by a reversed-phase column, Resolvex C18 (10 μm), 250 × 4.6 mm (Fisher Scientific Co., Pittsburg, PA) with acetonitrile-water (40:60) at a wavelength of 280 nm. The radioactive samples were mixed with the non-radioactive standard mixture solution to give the HPLC chromatograms. Each species was collected on a FOXY Fraction Collector (ISCO, Lincoln, NE) with mode 3 and cycle 0. The fraction collector was programmed to give fraction sizes based on the peak signals from the ISCO detector with a built-in peak separator. Each fraction was analyzed by liquid

scintillation counting. Steady-state fluxes were calculated using the following equations:

$$J_{2\beta,f} = \frac{\left(\frac{dA_{2\beta,R}}{dt}\right)}{S} \quad (10)$$

$$J_{1,f} = \frac{\left(\frac{dA_{1,R}}{dt}\right)}{S} \quad (11)$$

$$J_{1,b} = \frac{\left(\frac{dA_{1,D}}{dt}\right)}{S} \quad (12)$$

Here $J_{2\beta,f}$ and $J_{1,f}$ are the forward fluxes of $E_{2\beta}$ and E_1, and $J_{1,b}$ is the back flux of E_1, S is the effective diffusion area, $A_{2\beta,R}$ is the amount of $E_{2\beta}$ transported into the receiver chamber, $A_{1,R}$ and $A_{1,D}$ are the amounts of E_1 transported into the receiver and the donor chambers, respectively, and t is time. Normalized fluxes are defined as the fluxes given by Eqns 10–12 divided by the donor $E_{2\beta}$ concentration.

Eqns 10–12 may underestimate the correct fluxes because the amount of permeant retained in the epidermis/dermis is not negligible compared to the permeant in the receiver chamber. A procedure for correcting the flux values was recently developed (Liu, 1989; Liu et al., 1990) and it has been applied where necessary to the experimental data.

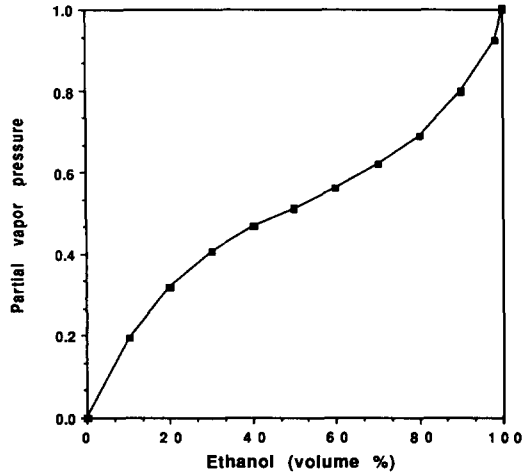

Fig. 3. Partial vapor pressure of ethanol in ethanol/water mixtures at 37 °C.

Solubilities of $E_{2\beta}$ and E_1 in ethanol/saline mixtures Solubilities of $E_{2\beta}$ and E_1 were determined, respectively, in ethanol/saline mixtures (for the 0–35% range of ethanol concentration). An excess amount of the compound was introduced into 1.5 ml polypropylene microcentrifuge tubes with different ethanol/saline mixtures and sealed with parafilm. The tubes were shaken for 72 h at 37 °C in a thermostatically controlled water bath and then centrifuged at 2000 rpm for 5 min. The clear supernatant solution was diluted appropriately and analyzed by HPLC.

Results and Discussion

Input information to be used in analysis of the asymmetric experiments

In this section, we will present and discuss the input parameters which will be used in the asymmetric flux predictions with Eqn 6. These predictions are for both ethanol transport and the cotransport of ethanol and $E_{2\beta}$ in stripped skin and full-thickness skin. Ethanol partial vapor pressure data (Washburn, 1928) were used to calculate the ratios of the partition coefficients for ethanol (see Eqn 6). These data are presented in Fig. 3. The ratios of the partition coefficients for $E_{2\beta}$ and for E_1 may be obtained from the solubility data (Ghanem et al., 1987). The pertinent solubility data for both drugs are shown in Fig. 4. Symmetric permeability coefficients for ethanol obtained from symmetric experiments are presented in Fig. 5. Most of the symmetric permeability coefficient data for $E_{2\beta}$ and E_1 were obtained previously (Liu et al., 1990, 1991) and these are summarized in Fig. 6. Ethanol inhibition of the enzymatic conversion of $E_{2\beta}$ to E_1 in hairless mouse skin has been observed as a decrease in the apparent enzyme rate constant, k, with increasing ethanol concentration (Liu et al., 1991). Fig. 7 presents a plot of k vs ethanol concentrations.

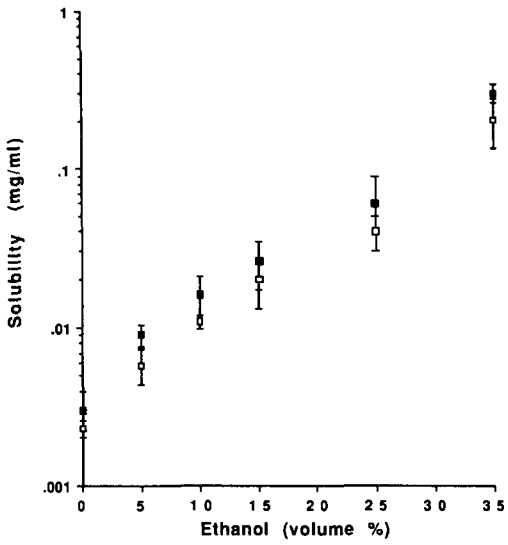

Fig. 4. Solubility of $E_{2\beta}$ (closed symbol) and of E_1 (open symbol) in ethanol/saline mixtures. Each point represents the mean ± S.D. of eight determinations.

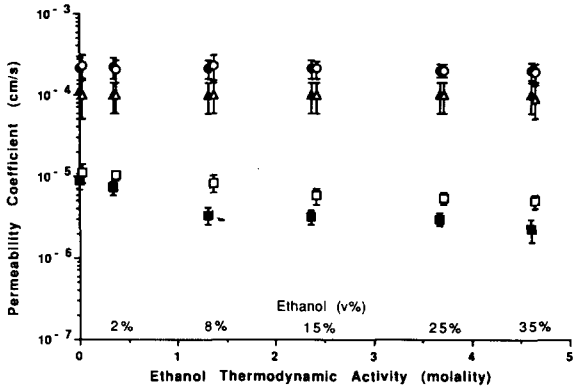

Fig. 6. Permeability coefficients of $E_{2\beta}$ (closed symbols) and E_1 (open symbols) in dermis (triangle), epidermis (circle), and stratum corneum (square) as functions of ethanol activity (molality scale) and ethanol concentration (v%) in the symmetric situation. Each point represents the mean ± S.D. of four determinations. Ethanol activity is proportional to the partial vapor pressure.

Ethanol fluxes and ethanol gradients for the steady-state asymmetric situation

Dermis and stripped skin Table 1 presents the results of comparisons between asymmetric experiments and theoretical predictions for the dermis and stripped skin at 2 and 8% ethanol. Here the fluxes are presented as normalized fluxes, i.e., the fluxes divided by the donor chamber concentration. As can be seen, there is good agreement between experiment and theory for the dermis and the stripped skin cases.

Fig. 8 gives the theoretically calculated ethanol concentration gradients for the stripped skin cases of Table 1. As can be seen, the individual concentration gradients are nearly linear and this is a

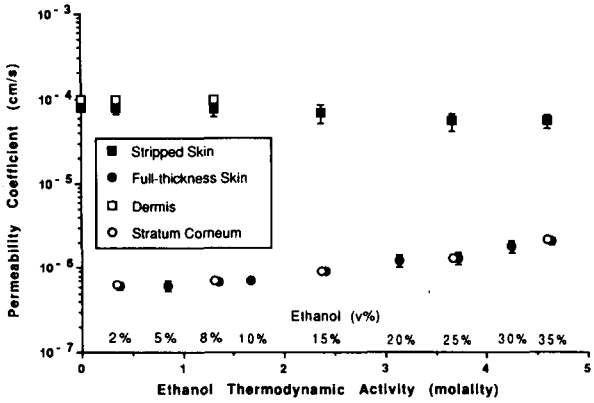

Fig. 5. Ethanol permeability coefficients in hairless mouse epidermis, dermis, stripped skin, stratum corneum, and full-thickness skin as functions of ethanol activity (molality scale) and ethanol concentration (v%) in the symmetric situation. Each point represents the mean ± S.D. of two to three determinations. Ethanol activity is proportional to the partial vapor pressure.

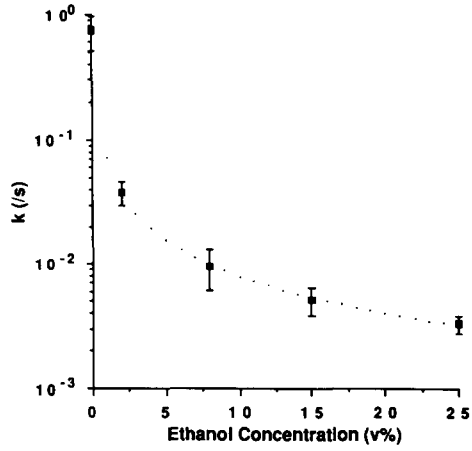

Fig. 7. Ethanol effect on the intrinsic first-order enzyme rate constant in the basal layer of epidermis with $E_{2\beta}$. Each data point represents the mean ± S.D. of 16 determinations. The dotted line is the best-fit curve of the competitive inhibition kinetics with an inhibition constant value of 0.10%.

TABLE 1

Normalized ethanol fluxes with dermis and stripped skin in the asymmetric situation: comparisons between experimental and theory [a]

Ethanol (donor/receiver) (v%)		Normalized flux (cm/s)($\times 10^5$)	
		Dermis	Stripped skin
2/0	Experimental	10.0 ± 1.00	9.00 ± 1.50
	Theory	9.80	8.54
8/0	Experimental		8.85 ± 1.01
	Theory		8.13

[a] The experimental normalized fluxes are expressed as the mean ± S.D. ($n = 3$). Theoretical fluxes were calculated using the procedure involving Eqn 6 and the mean values of the data in Figs 3 and 5. The information in Fig. 3 was used to calculate the ratios of the partition coefficients using the following relations,

$$\frac{K_{i,l}}{K_i} = \frac{\left(\frac{p_{i,l}}{p_i}\right)}{\left(\frac{C_{i,l}}{C_i}\right)} \quad \text{and} \quad \frac{K_{i,r}}{K_i} = \frac{\left(\frac{p_{i,r}}{p_i}\right)}{\left(\frac{C_{i,r}}{C_i}\right)}$$

where $p_{i,l}$, p_i, and $p_{i,r}$ are the ethanol partial vapor pressures at the left side, in the middle, and at the right side of element i. Fig. 5 was used to provide the dermis permeability coefficient of $P_d = 9.9 \times 10^{-5}$ cm/s and the epidermis permeability coefficient of $P_e = 7.4 \times 10^{-4}$ cm/s. These numbers were then in turn used to give the P_i values,

$$P_{i(\text{dermis})} = nP_d \quad \text{and} \quad P_{i(\text{epid.})} = nP_e$$

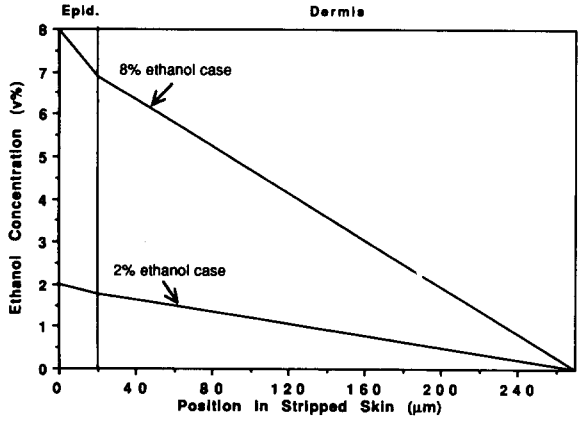

Fig. 8. Ethanol gradients (v%) across stripped hairless mouse skin for the asymmetric situations of 2 and 8% ethanol, calculated with the mean values of the symmetric ethanol parameters.

TABLE 2

Normalized ethanol fluxes with full-thickness skin in the asymmetric situation: comparisons between experimental and theory [a]

Ethanol (donor/receiver) (v%)	Normalized flux (cm/s)	
	Experimental	Theory
25/0	$(7.12 \pm 1.36) \times 10^{-7}$	6.18×10^{-7}
35/0	$(8.71 \pm 1.71) \times 10^{-7}$	6.87×10^{-7}

[a] The experimental normalized fluxes are expressed as the mean ± S.D. ($n = 4$). Theoretical fluxes were calculated using the procedure involving Eqn 6 and the mean values of the data in Figs 3 and 5. The information in Fig. 3 was used to calculate the ratios of the partition coefficients using the following relations,

$$\frac{K_{i,l}}{K_i} = \frac{\left(\frac{p_{i,l}}{p_i}\right)}{\left(\frac{C_{i,l}}{C_i}\right)} \quad \text{and} \quad \frac{K_{i,r}}{K_i} = \frac{\left(\frac{p_{i,r}}{p_i}\right)}{\left(\frac{C_{i,r}}{C_i}\right)}$$

where $p_{i,l}$, p_i, and $p_{i,r}$ are the ethanol partial vapor pressures at the left side, in the middle, and at the right side of element i. Fig. 5 was used to provide the permeability coefficients for dermis (P_d), epidermis (P_e), and stratum corneum (P_{sc}). These numbers were then in turn used to give the P_i values,

$$P_{i(\text{dermis})} = nP_d, \quad P_{i(\text{epid.})} = nP_e, \quad \text{and} \quad P_{i(\text{s.c.})} = nP_{sc}$$

consequence of (a) the P_i values being relatively constant within both the dermis and epidermis (Fig. 5) and (b) the ratios of the partition coefficients being all close to unity (i.e., Henry's Law is obeyed) in this low ethanol concentration range.

Full thickness skin Table 2 and Fig. 9 present the results of the asymmetric ethanol transport studies with full-thickness skin at 25 and 35% ethanol concentrations. Table 2 shows there is a good agreement between experiment and theory for both the 25 and 35% ethanol cases. The experiments and theory are essentially in agreement within experimental error. As it is instructive to see how the parameters in Eqn 6 may vary with position in the stratum corneum, this information is presented in the Appendix.

These results may be interpreted to mean that the approach involved is sound and the resulting ethanol concentration profiles in the hypothetical aqueous layers (Fig. 9) may now be used in the analyses of the $E_{2\beta}$ transport data.

TABLE 3

Normalized fluxes for $E_{2\beta}$ and E_1 in the simultaneous diffusion and metabolism of $E_{2\beta}$ with stripped skin in the asymmetric situation: comparisons between experimental and theory [a]

Ethanol (donor/receiver) (v%)		Normalized flux (cm/s)($\times 10^5$)		
		$J_{2\beta,f}/C_{2\beta,D}$	$J_{1,f}/C_{2\beta,D}$	$J_{1,b}/C_{2\beta,D}$
2/0	Experimental	6.89 ± 1.36	0.62 ± 0.28	1.83 ± 0.81
	Theory	6.71	0.55	1.70
8/0	Experimental	8.41 ± 1.78	0.15 ± 0.06	0.42 ± 0.15
	Theory	8.10	0.18	0.39

[a] The experimental normalized fluxes are expressed as the mean ± S.D. ($n = 4$). Theoretical fluxes were calculated using the procedure involving Eqns 6–8 and the mean values of the data in Figs 4 and 6–8. All of the parameter values were assigned based on the ethanol gradients in Fig. 8. Fig. 4 was used to calculate the ratios of the partition coefficients using the following relations:

$$K_{i,l}/K_i = S_i/S_{i,l} \quad \text{and} \quad K_{i,r}/K_i = S_i/S_{i,r}$$

where $S_{i,l}$, S_i, and $S_{i,r}$ are the solubilities of $E_{2\beta}$ or E_1 in the aqueous ethanol solutions corresponding to the left side, the middle, and the right side of element i. Fig. 6 was used to provide the permeability coefficients for dermis (P_d) and epidermis (P_e). These numbers were then in turn used to give the P_i values:

$$P_{i(\text{dermis})} = nP_d \quad \text{and} \quad P_{i(\text{epid.})} = nP_e$$

The information in Fig. 7 was used to calculate the ethanol concentration-dependent (or position-dependent) apparent enzyme rate constant in the basal layer of the epidermis.

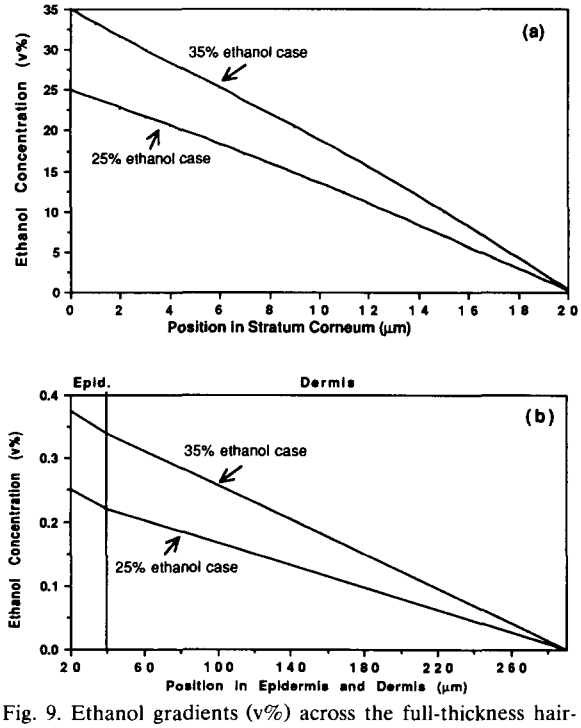

Fig. 9. Ethanol gradients (v%) across the full-thickness hairless mouse skin for the asymmetric situation of 25 and 35%, calculated with the mean values of the symmetric ethanol parameters. (a) For stratum corneum (the hypothetical aqueous layers); (b) for epidermis (Epid.) and dermis.

Simultaneous diffusion and metabolism of $E_{2\beta}$ for the asymmetric situation

Stripped skin Table 3 and Fig. 10 give the results of the $E_{2\beta}$ transport and metabolism in stripped skin for the 2 and 8% asymmetric ethanol

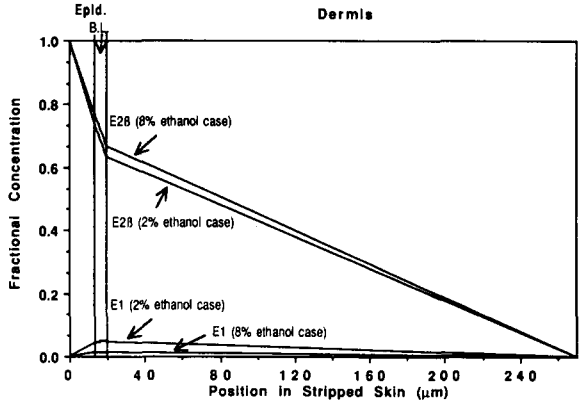

Fig. 10. Fractional concentration gradients of $E_{2\beta}$ and E_1 in stripped hairless mouse skin in the simultaneous diffusion and metabolism of $E_{2\beta}$ for the asymmetric situations of 2 and 8% ethanol, calculated with the linear ethanol gradients in epidermis and in dermis and the mean values of the symmetric parameters of $E_{2\beta}$ and E_1. Epid., epidermis; B.L., basal layer of the epidermis.

situations. The experimental fluxes were calculated using Eqns 10–12 and these are presented as normalized fluxes in Table 3. The theoretical predictions were made taking into account the ethanol gradient (Fig. 8), its influence upon the enzyme rate constant, k (Fig. 7), and its effect upon the ratio of partition coefficients obtained from the solubility data (Fig. 4). Also, it was necessary to use Eqns 7 and 8 instead of Eqn 6 for the basal layer region that describes simultaneous $E_{2\beta}$ position-dependent diffusion and metabolism.

The agreement between experimental results and theoretical predictions is very good for all fluxes and for the two ethanol levels. This outcome strongly supports the validity of the calculational approach as the input data were quite independent of the asymmetric experiments.

Full-thickness skin Table 4 compares the experimental fluxes for the 25 and 35% ethanol cases with the theoretical predictions. As for the stripped skin case, Eqns 10–12 were used to calculate the normalized fluxes. The theoretical fluxes were calculated with Eqns 6–8 using the ethanol gradient data (Fig. 9), the permeability coefficient data (Fig. 6), the solubility data (Fig. 4), and the enzyme rate constant data (Fig. 7). As can be seen, the agreement between the experimental and theoretical fluxes may be considered to be quite satisfactory in view of the many factors involved in the calculations. The position-dependent permeability coefficients and ratios of partition coefficients for $E_{2\beta}$ and for E_1 are given in the Appendix where 10 elements were used in the calculation with Eqns 6–8.

Figs 11–13 present the fractional concentration profiles of $E_{2\beta}$ and E_1 for the 25 and 35% cases. These informative plots show the expected relationship between $E_{2\beta}$ and E_1 in the stratum corneum (concentrations in the hypothetical aqueous ethanol layers), epidermis, and dermis. Both compounds show linear profiles in the dermis. In the basal layer region, there is considerable nonlinearity that arises because of the metabolism in this region. Another noteworthy point is that the E_1-to-$E_{2\beta}$ concentration ratios

TABLE 4

Normalized fluxes for $E_{2\beta}$ and E_1 in the simultaneous diffusion and metabolism of $E_{2\beta}$ with full-thickness skin in the asymmetric situation: comparisons between experimental and theory [a]

Ethanol (donor/receiver) (v%)		Normalized flux (cm/s)($\times 10^7$)		
		$J_{2\beta,f}/C_{2\beta,D}$	$J_{1,f}/C_{2\beta,D}$	$J_{1,b}/C_{2\beta,D}$
25/0	Experimental	2.98 ± 1.32	3.97 ± 1.59	0.78 ± 0.35
	Theory	2.33	3.62	0.84
35/0	Experimental	2.03 ± 0.84	2.12 ± 0.74	0.31 ± 0.16
	Theory	1.25	1.45	0.43

[a] The experimental normalized fluxes are expressed as the mean ± S.D. ($n = 4$). Theoretical fluxes were calculated using the procedure involving Eqns 6–8 and the mean values of the data in Figs 9, 4, 6, and 8. All of the parameter values were assigned based on the ethanol gradients in Fig. 9. Fig. 4 was used to calculate the ratios of the partition coefficients using the following relations:

$$K_{i,l}/K_i = S_i/S_{i,l} \quad \text{and} \quad K_{i,r}/K_i = S_i/S_{i,r}$$

where $S_{i,l}$, S_i, and $S_{i,r}$ are the solubilities of $E_{2\beta}$ or E_1 in the aqueous ethanol solutions corresponding to the left side, the middle, and the right side of element i. Fig. 6 was used to provide the permeability coefficients for dermis (P_d), epidermis (P_e), and stratum corneum (P_{sc}). These numbers were then in turn used to give the P_i values:

$$P_{i(\text{dermis})} = nP_d; \quad P_{i(\text{epid.})} = nP_e; \quad \text{and} \quad P_{i(\text{s.c.})} = nP_{sc}$$

The information in Fig. 7 was used to calculate the ethanol concentration-dependent (or position-dependent) apparent enzyme rate constant in the basal layer of the epidermis.

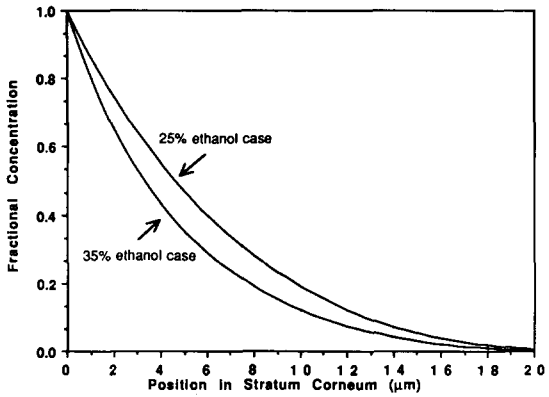

Fig. 11. Fractional concentration gradients for $E_{2\beta}$ in hairless mouse stratum corneum (the hypothetical aqueous layers) during simultaneous diffusion and metabolism of $E_{2\beta}$ for the asymmetric situations of 25 and 35% ethanol.

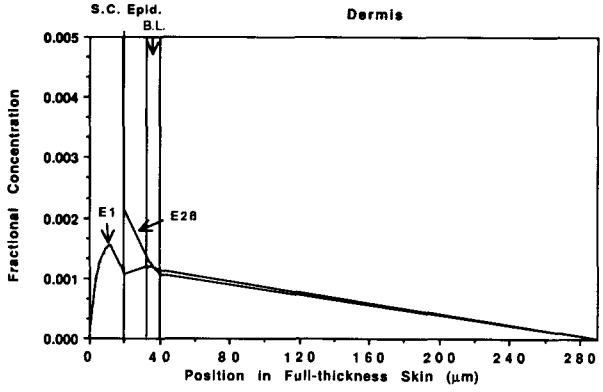

Fig. 13. Fractional concentration gradients of $E_{2\beta}$ and E_1 in full-thickness hairless mouse skin during simultaneous diffusion and metabolism of $E_{2\beta}$ for the asymmetric case of 35% ethanol. S.C., stratum corneum (the hypothetical aqueous layers); Epid., epidermis; B.L., basal layer of the epidermis.

for the 25% case are generally somewhat higher than those for the 35% case; this is consistent with information in Fig. 9b which shows the significantly higher ethanol levels in the basal layer for the 35% case. It is seen that the concentration profiles for $E_{2\beta}$ in the stratum corneum (the hypothetical aqueous layers) are concave upwards and the back diffusion of E_1 gives rise to a peak in E_1 concentration profile in the stratum corneum (the hypothetical aqueous layers).

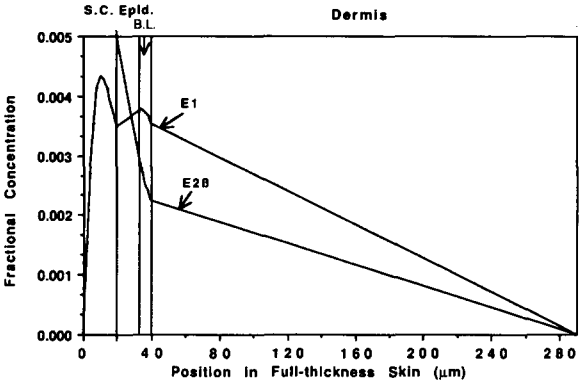

Fig. 12. Fractional concentration gradients of $E_{2\beta}$ and E_1 in full-thickness hairless mouse skin during simultaneous diffusion and metabolism of $E_{2\beta}$ for the asymmetric situation of 25% ethanol. S.C., stratum corneum (the hypothetical aqueous layers); Epid., epidermis; B.L., basal layer of the epidermis.

Additional comments on the calculational method

When the asymmetric problem was first considered, attempts were made to involve explicitly the permeant diffusion coefficient (D) and the permeant partition coefficient (K) in the analysis of the data. These D and K values were to be functions of the ethanol concentration and therefore of position in the stratum corneum, epidermis, and dermis. It soon became apparent, however, that this approach would at best require an enormous number of independent experiments; also, the physical meanings of the D and K values would be unclear as we would not be dealing with homogeneous skin membrane layers (stratum corneum, epidermis, and dermis).

The present approach of hypothetically slicing the stratum corneum, epidermis, and dermis into thin elements separated by the aqueous/ethanol solution appropriate for the particular steady-state situation greatly simplifies solving the asymmetric problem. Fortunately, both P_i and K_i ratios are known from independent experiments. Also fortunately, the ethanol flux and concentration gradient problem is solved using the same equation (Eqn 6) as for the $E_{2\beta}/E_1$ situation.

Perhaps, a key assumption made in the present approach is that all of the n elements of the stratum corneum may be assigned the P/n value based upon the experimental P value for the full stratum corneum when the ethanol activity is

known. This assumption is equivalent to stating that the transport property of the stratum corneum is independent of depth in the stratum corneum. The reasonably good agreement between experiment and theory (Tables 2 and 4) strongly suggests that the assumption may be a good one or, at least, there may be some cancellation/compensation of the errors.

It is believed that the physical model approach presented here for analyzing the asymmetric situation should be of value in designing/optimizing transdermal delivery system formulations and in understanding their performance in the in vivo situation (i.e., the drug formulation on one side of the skin and aqueous physiological solution on the other side).

Appendix

An example of the stratum corneum position-dependent permeability coefficients, ratios of partition coefficients, and concentrations of ethanol, $E_{2\beta}$, and E_1

As it is instructive to see how the parameters in Eqn 6 may vary with position in the stratum corneum, information is presented in Tables 5–7 for ethanol, $E_{2\beta}$, and E_1, respectively, for the

TABLE 5

Permeability coefficients, ratios of partition coefficients, and concentrations of ethanol across stratum corneum in ethanol transport through full-thickness skin for the asymmetric situation (25%) [a]

i	$C_{i,l}$ (v%)	$C_{i,r}$ (v%)	P_i (cm/s)	$K_{i,l}/K_i$	$K_{i,r}/K_i$
1	25.00	22.82	1.46×10^{-5}	0.977	1.024
2	22.82	20.60	1.31×10^{-5}	0.977	1.024
3	20.60	18.32	1.17×10^{-5}	0.976	1.025
4	18.32	15.96	1.04×10^{-5}	0.975	1.026
5	15.96	13.52	9.26×10^{-6}	0.974	1.026
6	13.52	10.97	8.25×10^{-6}	0.973	1.026
7	10.97	8.33	7.40×10^{-6}	0.972	1.028
8	8.33	5.62	6.73×10^{-6}	0.971	1.029
9	5.62	2.90	6.27×10^{-6}	0.971	1.030
10	2.90	0.25	6.04×10^{-6}	0.972	1.029

[a] Eqn 6 was used for this calculation when P_i, $K_{i,l}/K_i$, and $K_{i,r}/K_i$ were known as functions of the aqueous ethanol concentration (Figs 3 and 5). The concentrations refer to the hypothetical aqueous ethanol layers (Fig. 9).

TABLE 6

Permeability coefficients, ratios of partition coefficients, and concentrations of $E_{2\beta}$ in the stratum corneum for the simultaneous transport and metabolism of $E_{2\beta}$ with full-thickness skin for the asymmetric situation (25%) [a]

i	$C_{i,l}$	$C_{i,r}$	P_i (cm/s)	$K_{i,l}/K_i$	$K_{i,r}/K_i$
1	1.000	0.748	3.05×10^{-5}	0.876	1.141
2	0.748	0.552	3.10×10^{-5}	0.874	1.144
3	0.552	0.400	3.15×10^{-5}	0.871	1.148
4	0.400	0.282	3.20×10^{-5}	0.867	1.154
5	0.282	0.191	3.25×10^{-5}	0.862	1.160
6	0.191	0.123	3.30×10^{-5}	0.857	1.167
7	0.123	0.072	3.40×10^{-5}	0.852	1.174
8	0.072	0.038	4.00×10^{-5}	0.848	1.179
9	0.038	0.017	5.83×10^{-5}	0.848	1.179
10	0.017	0.005	7.95×10^{-5}	0.851	1.175

[a] Eqns 6–8 were used for this calculation when P_i, $K_{i,l}/K_i$, and $K_{i,r}/K_i$ were known as functions of the aqueous ethanol concentration (Figs 4 and 5). The (fractional) concentrations correspond to the hypothetical aqueous layers (Fig. 12).

TABLE 7

Permeability coefficients, ratios of partition coefficients, and concentrations of E_1 in the stratum corneum for the simultaneous transport and metabolism of $E_{2\beta}$ with full-thickness skin for the asymmetric situation (25%) [a]

i	$C_{i,l}$	$C_{i,r}$	P_i (cm/s)	$K_{i,l}/K_i$	$K_{i,r}/K_i$
1	0.00000	0.00133	5.55×10^{-5}	0.877	1.140
2	0.00133	0.00232	5.65×10^{-5}	0.873	1.145
3	0.00232	0.00305	5.70×10^{-5}	0.872	1.148
4	0.00305	0.00356	5.78×10^{-5}	0.868	1.153
5	0.00356	0.00386	5.95×10^{-5}	0.861	1.161
6	0.00386	0.00390	6.85×10^{-5}	0.857	1.167
7	0.00390	0.00373	8.00×10^{-5}	0.852	1.174
8	0.00373	0.00348	9.00×10^{-5}	0.848	1.179
9	0.00348	0.00322	9.90×10^{-5}	0.848	1.180
10	0.00322	0.00300	1.09×10^{-4}	0.851	1.175

[a] Eqns 6–8 were used for this calculation when P_i, $K_{i,l}/K_i$, and $K_{i,r}/K_i$ were known as functions of the aqueous ethanol concentration (Figs 4 and 5). The concentrations (normalized by the $E_{2\beta}$ donor concentration) correspond to the hypothetical aqueous layers (Fig. 12).

25% ethanol case when 10 elements of stratum corneum were used in the calculation.

Acknowledgements

This research was supported by the Ciba-Geigy Corp. (Ardsley, NY). P.L. was supported in part by the University of Utah Graduate Research Fellowship (1987–1988).

References

Durrheim, H., Flynn, G.L., Higuchi, W.I. and Behl, C.R., Permeation of hairless mouse skin. I. experimental methods and comparison with human epidermal permeation by alkanols. *J. Pharm. Sci.*, 69 (1980) 781–786.

Ghanem, A.H., Mahmoud, H., Higuchi, W.I., Rohr, U.D., Borsadia, S., Liu, P., Fox, J.L. and Good, W.R., The effects of ethanol on the transport of β-estradiol and other permeants in hairless mouse skin. II. a new quantitative approach. *J. Cont. Rel.*, 6 (1987) 75–83.

Higuchi, W.I., Fox, J.L., Knutson, K., Anderson, B.D. and Flynn, G.L., The dermal barrier to local and systemic drug delivery. In Repta A.J. and Stella, V.J. (Eds), *Directed Drug Delivery*, Humana Press, Clifton, NJ, 1985, pp. 97–117.

Higuchi, W.I., Rohr, U.D., Burton, S.A., Liu, P., Fox, J.L., Ghanem, A.H., Mahmoud, H., Borsadia, S. and Good, W.R., The effect of ethanol on the transport of β-estradiol in hairless mouse skin: I. comparison of experimental data with a pore model. In Lee, P.I. and Good, W.R. (Eds), *Controlled Release Technology, Pharmaceutical Applications*, ACS Symp. Ser. 348, Am. Chem. Soc., Washington, DC, 1987, pp. 232–240.

Kurihara-Bergstrom, T., Flynn, G.L. and Higuchi, W.I., Physicochemical study of percutaneous absorption enhancement by dimethyl sulfoxide: kinetic and thermodynamic determinants of dimethyl sulfoxide. *J. Pharm. Sci.*, 75 (1980) 479–486.

Liu, P., The Influences of Ethanol on Simultaneous Diffusion and Metabolism of β-Estradiol in Skin, Ph.D. Thesis, The University of Utah, Salt Lake City (1989).

Liu, P., Higuchi, W.I., Ghanem, A.H., Kurihara-Bergstrom, T. and Good, W.R., Quantitation of simultaneous diffusion and metabolism of β-estradiol in hairless mouse skin: enzyme distribution and intrinsic diffusion/metabolism parameters. *Int. J. Pharm.*, 64 (1990) 7–25.

Liu, P., Higuchi, W.I., Song, W., Kurihara-Bergstrom, T. and Good, W.R., Quantitative evaluation of ethanol effects on diffusion and metabolism of β-estradiol in hairless mouse skin. *Pharm. Res.*, 8 (1991) 865–872.

Mollgaard, B. and Hoelgaard, A., Vehicle effect on topical drug delivery: I. influence of glycols and drug concentration on skin transport. *Acta Pharm. Suec.*, 20 (1983a) 433–442.

Mollgaard, B. and Hoelgaard, A., Vehicle effect on topical drug delivery: II. concurrent skin transport of drugs and vehicle component. *Acta Pharm. Suec.*, 20 (1983b) 443–450.

Poulsen, B.J., Diffusion of drugs from topical vehicles: an analysis of vehicle effects. In Montagna, W., Van Scott, E.J. and Stoughton, R.B. (Eds), *Pharmacology and the Skin*, Meredith, New York, 1972, pp. 495–510.

Sarpotdar, P., Gaskill, J.L. and Giannini, R.P., Effect of polyethylene glycol 400 on the penetration of drugs through human skin in vitro. *J. Pharm. Sci.*, 75 (1986) 26–28.

Schaefer, H., Schalla, W., Gazith, J., Stuttgen, G. and Bauer,

E., Principles of percutaneous absorption. In Turner, P. (Ed.), *Clinical Pharmacology and Therapeutics*, University Park Press, Baltimore, 1981, pp. 396–403.

Sloan, K.B., Silver, K.G. and Koch, S.A.M., The effect of vehicle on the diffusion of salicylic acid through hairless mouse skin. *J. Pharm. Sci.*, 75 (1986) 744–749.

Stehle, R.G. and Higuchi, W.I., In vitro model for transport of solutes in three phase system II. experimental considerations. *J. Pharm. Sci.*, 61 (1972) 1931–1937.

Washburn, E.W., *International Critical Tables of Numerical Data, Physics, Chemistry and Technology*, Vol. III, McGraw-Hill, New York, 1928, p. 361.

Yu, C.D., Fox, J.L., Ho, N.F.H. and Higuchi, W.I., Physical model evaluation of topical prodrug delivery – simultaneous transport and bioconversion of vidarabine-5′-valerate II. parameter determination. *J. Pharm. Sci.*, 68 (1979) 1347–1357.